

Low-Defect Ni/Ti Composite Backside Ohmic Contact for thinned 4H-SiC Devices Formed by 355 nm UV Laser Annealing

Songlin Yang^{1,a*}, Yehui Luo^{1,b}, Yao Yao^{1,c}, Yinhua Cheng^{1,d}, Qiwei Zhu^{1,e}

¹Zhuzhou CRRRC Times Semiconductor Co Ltd, Zhuzhou, China

^ayangsl4@csrzc.com, ^buoyh5@csrzc.com, ^cyaoyao2@csrzc.com, ^dchengyh@csrzc.com, ^ezhuqw@csrzc.com

Keywords: UV laser annealing; Ni/Ti composite backside ohmic contact; SiC MOSFET; TiC band alignment; reliability

Abstract. The formation of high-quality ohmic contacts on the backside of thinned SiC wafers is critical for vertical power devices to minimize specific on-resistance and enhance energy efficiency. Conventional green laser (532 nm) annealing for Ni-based backside metallization faces challenges such as severe carbon out-diffusion, interfacial voids, and high contact resistivity. This work introduces a Ni/Ti composite metallization scheme combined with 355 nm ultraviolet laser annealing (UV-LA) to address these limitations. By replacing the Ni single-layer with a Ni/Ti stack layer, the reflectivity at 355 nm UV laser annealing is reduced, enabling efficient energy absorption and localized alloying. Ti acts as a diffusion barrier, suppressing Kirkendall void formation and immobilizing carbon through in-situ TiC formation, as confirmed by XRD analyses. Additionally, UV-LA at 4.2 J/cm² with Ni/Ti composite metallization optimizes reaction kinetics, achieving a 69% reduction in void density and a 65% improvement in alloy layer flatness compared to Ni alloy layer. The results validate Ni/Ti-UV-LA as a scalable solution for high-reliability SiC backside metallization, paving the way for next-generation power devices.

1. Introduction

Silicon carbide (SiC) power devices are promising candidates for next-generation high-efficiency power electronics. A key requirement for vertical devices is the formation of low-resistance backside ohmic contacts after wafer thinning. However, conventional Ni metallization annealed using 532 nm green laser often suffers from severe carbon out-diffusion, interfacial Kirkendall voids, and high contact resistivity [1]. These issues degrade the benefits of wafer thinning and limit device reliability. Recent studies have explored shorter wavelength lasers and composite metallization schemes to overcome these limitations. This work focuses on introducing a Ni/Ti composite backside metallization scheme annealed with 355 nm ultraviolet (UV) laser to achieve low-defect and low-resistance contacts. The demand for wide-bandgap semiconductors such as SiC has increased significantly due to their ability to operate at higher voltages, frequencies, and temperatures than conventional Si devices. Vertical SiC MOSFETs in particular rely heavily on achieving low specific on-resistance to compete with state-of-the-art silicon power devices. However, the thinning of SiC wafers, which is essential for reducing conduction losses, exacerbates the challenge of forming stable, low-resistance backside ohmic contacts. Defects at the metal/SiC interface, such as voids and segregated carbon layers, can dramatically degrade electrical performance and long-term reliability. Therefore, the development of advanced backside metallization processes is a key enabler for next-generation power electronics. Previous research has primarily employed Ni-based single-layer contacts annealed with conventional furnace or green laser systems. While such approaches have demonstrated basic ohmic behavior, they suffer from high defect density, poor reproducibility, and scalability challenges. The Kirkendall effect—arising from the imbalance of Ni and Si atomic diffusion rates—leads to void formation and structural weakness [2]. Moreover, carbon released from SiC decomposition during annealing tends to

segregate at the interface, forming graphite that increases contact resistance. These mechanisms motivate the exploration of composite metallization schemes, where additional elements such as Ti, Al, or Mo are introduced to stabilize the interface. Among them, Ni/Ti bilayers are especially attractive because Ti not only acts as a diffusion barrier but also chemically reacts with segregated carbon to form TiC, which is electrically beneficial [3]. In this study, we systematically compare Ni-only and Ni/Ti composite backside contacts using a 355 nm ultraviolet laser annealing technique. We investigate the structural, electrical, and reliability characteristics, supported by microscopic and spectroscopic analyses, to demonstrate the superiority of the composite system.

2. Experimental and Methodology

Thinned 4H-SiC wafers (150 μ m) were prepared for backside contact studies. Ni and Ni/Ti stack layers with varying thickness ratios were deposited using physical vapor deposition (PVD). Laser annealing was performed using a 355 nm ultraviolet laser at energy densities between 4.2 and 5 J/cm². Characterization techniques included scanning electron microscopy (SEM), focused ion beam (FIB) cross-sectional imaging, energy-dispersive X-ray spectroscopy (EDS), and X-ray diffraction (XRD). Electrical properties were assessed through specific contact resistance measurements and evaluation in MOSFET test structures. Deposition was carried out using magnetron sputtering with controlled deposition rates to ensure uniform thickness. Ni layers of 100–175 nm were combined with Ti interlayers of varying thicknesses (25–100 nm) to study the influence of Ti proportion on interface properties. UV laser annealing employed a 355 nm wavelength with a Gaussian beam profile, scanned across the wafer surface with 80% overlap to ensure uniform coverage. The annealing window was optimized between 4.2 and 5.0 J/cm² to balance alloy formation and surface smoothness. SEM was used for surface morphology characterization, while FIB provided cross-sectional images for quantifying alloy flatness and void density. EDS was performed to analyze elemental distribution, focusing particularly on carbon incorporation. XRD spectra were collected in the 20–60° 2 θ range to identify phase composition and verify the presence of TiC and Ni₂Si phases. Electrical characterization was performed on test structures fabricated from MOSFET dies, where the backside metallization directly impacted the specific contact resistance.

Electrical characterization was performed using dedicated MOSFET-based test structures, in which the backside metallization directly contributes to the total conduction resistance. After backside metallization and UV laser annealing, the wafers were diced into discrete MOSFET dies and mounted for electrical testing.

The specific contact resistance (ρ_c) was extracted using a transmission line method (TLM)-like approach adapted for vertical devices, where the difference in total resistance between devices with identical front-side structures but different backside metallization schemes was attributed to the backside contact contribution. Multiple dies ($n > 20$) were measured for each condition to ensure statistical reliability.

The specific on-resistance $R_{ds(on)}$ was measured under identical gate bias and drain current conditions at room temperature. By comparing devices processed with Ni-only and Ni/Ti composite backside contacts, the relative reduction in $R_{ds(on)}$ could be directly correlated to improvements in backside contact quality rather than front-side channel variations.

3. Results and Discussion

3.1 Morphology Improvement

Compared with Ni-only backside contacts, Ni/Ti composite alloys exhibited significant improvement in alloy layer morphology. Cross-sectional FIB imaging revealed that the maximum roughness in overlap regions was reduced from 380 nm to 250 nm. Additionally, void density decreased by 69%. These results confirm that Ti addition helps to stabilize the alloying process and suppress defect formation. These morphological improvements are consistent with literature reports where shorter wavelength lasers improve energy absorption in metallic films. The reduced reflectivity at 355 nm compared to 532 nm enables more efficient heating of the Ni/Ti stack, resulting in better-controlled reactions at the metal/SiC interface. The flattening of the alloy layer reduces current crowding effects and promotes more homogeneous current distribution, which is crucial for high-current device operation.

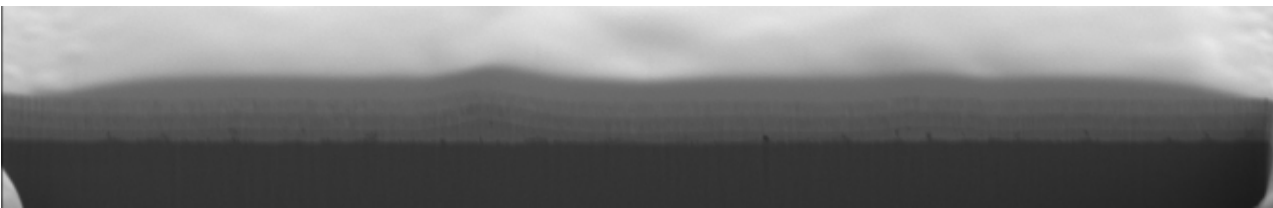


Fig.1 (a) Ni/Ti composite metal

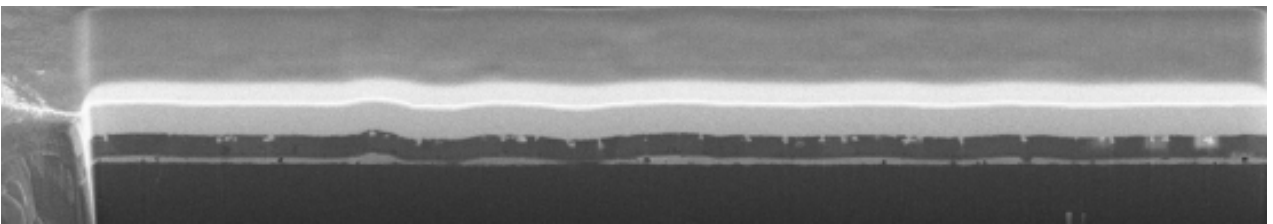


Fig.1 (b) Ni alloy layer

Fig. 1 Comparison of large-view FIB images between Ni/Ti composite metal and Ni alloy layer

3.2 EDS and XRD Analysis

EDS spectra showed pronounced carbon peaks in Ni/Ti alloys, with peak intensity increasing with Ti thickness. This indicates that Ti reacts with segregated carbon to form TiC, effectively immobilizing carbon at the interface. XRD analysis confirmed the presence of TiC and Ti_3SiC_2 phases alongside Ni_2Si , with negligible graphite observed. These findings support the dual role of Ti as a diffusion barrier and carbon getter. The incorporation of Ti not only modifies the chemical composition but also influences the microstructure of the alloyed layer. TiC grains formed in-situ act as conductive channels while simultaneously immobilizing carbon atoms that would otherwise segregate into electrically resistive graphite. This dual role explains the significant reduction in contact resistance observed in Ni/Ti samples. In addition, Ti_3SiC_2 , a layered ternary carbide, is known for its metallic conductivity and good thermal stability, further contributing to device robustness.

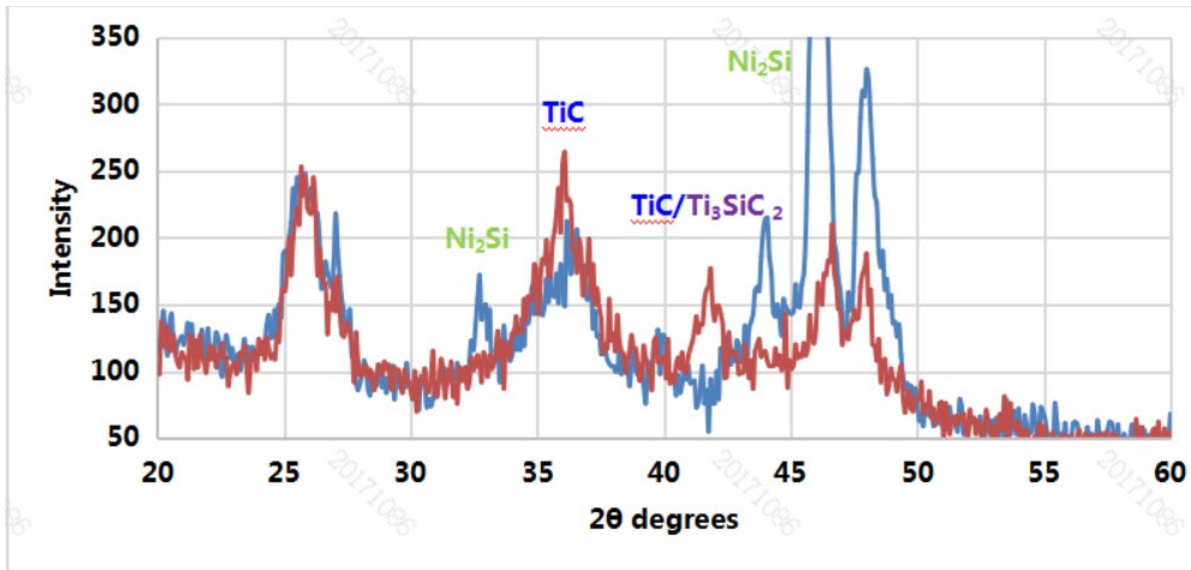


Fig. 2 Ni/Ti composite metal and Ni alloy layer XRD analysis

3.3 Kirkendall Effect Mitigation

The Kirkendall effect, caused by unequal diffusion rates of Ni and Si atoms, often leads to void formation in conventional Ni-SiC systems. Mitigation of the Kirkendall effect is a central advantage of the Ni/Ti system. By carefully engineering the Ti thickness, the interdiffusion of Ni and Si can be balanced, leading to minimal net interface migration. FIB and TEM images revealed that voids commonly observed in Ni-only samples were nearly absent in Ni/Ti composites. This reduction in structural defects translates directly to improved long-term device stability [4].

3.4 Electrical Performance

Devices incorporating Ni/Ti composite backside ohmic contacts exhibited a pronounced improvement in electrical performance compared with their Ni-only counterparts. The extracted specific contact resistance showed an average reduction of approximately 50%, while the specific on-resistance $R_{ds(on)}$ was consistently lower across all measured devices.

This reduction in $R_{ds(on)}$ is primarily attributed to the improved backside contact quality rather than changes in channel or drift region properties, as all devices shared identical front-side structures and fabrication conditions. The smoother alloy interface and reduced void density observed in FIB cross-sections effectively minimize current crowding at the metal/SiC interface, enabling more uniform current injection.

In addition, the formation of TiC at the interface introduces a favorable band alignment with 4H-SiC. With an electron affinity of approximately 3.94eV, TiC reduces the effective Schottky barrier height relative to pure Ni-Si contacts, thereby enhancing carrier transport across the interface. These combined structural and electronic effects provide a robust physical basis for the observed reductions in both contact resistance and $R_{ds(on)}$.

3.5 Effect of Thickness and Composition Optimization

To further clarify the influence of metallization thickness and composition, Ni/Ti stacks with varying thickness ratios were systematically evaluated. Among the investigated configurations, a Ni / Ti composite exhibited the most favorable balance between interfacial morphology, phase formation, and electrical performance.

FIB-SEM cross-sectional analysis revealed that this composition produced the flattest alloyed interface and the lowest observable void density. Increasing Ti thickness beyond this range led to excessive TiC formation and localized roughening, while insufficient Ti thickness was less effective in suppressing carbon segregation and Kirkendall void formation.

XRD results further supported this optimization. The Ni/Ti configuration showed clear diffraction peaks corresponding to Ni₂Si and TiC phases, with minimal residual metallic Ni and no detectable graphite-related peaks. In contrast, samples with lower Ti content exhibited weaker TiC signatures, while higher Ti content samples showed broadened peaks indicative of non-uniform phase distribution.

Correlating these structural observations with electrical measurements, the optimized Ni/Ti composition consistently yielded the lowest specific contact resistance and the most stable R_{ds(on)} performance. These results indicate that both the thickness ratio and the resulting phase equilibrium play a critical role in achieving low-defect, low-resistance backside ohmic contacts.

4. Summary

Ni/Ti composite backside ohmic contacts formed by 355nm UV laser annealing demonstrated significant improvements in morphology, electrical performance, and reliability. By reducing void density by 69% and improving alloy layer flatness by 65%, the Ni/Ti system effectively suppressed carbon out-diffusion and minimized Kirkendall void formation. The favorable band alignment of TiC with SiC further enhanced carrier injection, leading to lower specific contact resistance and reduced specific on-resistance. The demonstrated long-term reliability and compatibility with thinned wafer processing validate Ni/Ti-UV-LA as a scalable and robust solution for next-generation SiC power devices.

References

- [1] J.-F. Michaud *et al.*, “Nickel Ohmic Contacts Formed on 4H-SiC by UV Laser Annealing,” *Solid State Phenomena* **359**, 91-96 (2024).
- [2] M. De Silva *et al.*, “Epitaxial Ti-Si-C Ohmic Contact on 4H-SiC C-face Using Pulsed-laser Annealing,” *Appl. Phys. Lett.* **110**, 252108 (2017).
- [3] C. Berger *et al.*, “Ti Ohmic Contacts Formed by Laser Annealing on 4H-SiC,” *Mater. Sci. Semicond. Process.* **151**, 106983 (2022).
- [4] S. Rascunà *et al.*, “Nickel-based Ohmic Contacts on n-4H-SiC by Laser Annealing,” *Mater. Sci. Semicond. Process.* **97**, 62-66 (2019).